

Microfluidic Spinning of Cell-Responsive Grooved Microfibers

Xuetao Shi, Serge Ostrovidov, Yihua Zhao, Xiaobin Liang, Motohiro Kasuya, Kazue Kurihara, Ken Nakajima, Hojae Bae, Hongkai Wu,* and Ali Khademhosseini*

Engineering living tissues that simulate their natural counterparts is a dynamic area of research. Among the various models of biological tissues being developed, fiber-shaped cellular architectures, which can be used as artificial blood vessels or muscle fibers, have drawn particular attention. However, the fabrication of continuous microfiber substrates for culturing cells is still limited to a restricted number of polymers (e.g., alginate) having easy processability but poor cell–material interaction properties. Moreover, the typical smooth surface of a synthetic fiber does not replicate the micro- and nanofeatures observed in vivo, which guide and regulate cell behavior. In this study, a method to fabricate photocrosslinkable cell-responsive methacrylamide-modified gelatin (GelMA) fibers with exquisite microstructured surfaces by using a microfluidic device is developed. These hydrogel fibers with microgrooved surfaces efficiently promote cell encapsulation and adhesion. GelMA fibers significantly promote the viability of cells encapsulated in/or grown on the fibers compared with similar grooved alginate fibers used as controls. Importantly, the grooves engraved on the GelMA fibers induce cell alignment. Furthermore, the GelMA fibers exhibit excellent processability and could be wound into various shapes. These microstructured GelMA fibers have great potential as templates for the creation of fiber-shaped tissues or tissue microstructures.

the development of tissue engineering as an approach in regenerative medicine, micro- and nanoscale fibers have attracted interest for their potential use in engineered tissues or organs.^[2–7] One application of fibrous scaffolds is the engineering of microvessels, which ensure adequate nutrient delivery and carry waste products away from tissues and organs.^[8,9] Additionally, to simulate the hierarchical fibrous construction of human tissues, cell-laden microfibers have been used to design biomimetic scaffolds for the regeneration of skin, neuronal and cardiac tissues.^[10–12]

Recently, a variety of methods (e.g., electrospinning, wet spinning, interface complexation) have been used to produce cell-laden polymer/hydrogel fibers.^[13–16] However, these approaches can only generate cylindrical fibers or nanoscale fiber mats. This limitation provides an impetus to develop alternative techniques to create fibers with a topographical architecture that better recapitulates the complex structures and functions of living tissues or organs. A number of advances have been made in this area as a result of progress in microfluidic technology. Compared with other platforms, microfluidic techniques provide unprecedented opportunities to create microscale fibers with various morphologies (e.g.,

1. Introduction

Artificial and natural fibers have been spun or woven into a considerable number of industrial and consumer products, including garments, cords, and wound dressings.^[1] Due to

structures and functions of living tissues or organs. A number of advances have been made in this area as a result of progress in microfluidic technology. Compared with other platforms, microfluidic techniques provide unprecedented opportunities to create microscale fibers with various morphologies (e.g.,

Prof. X. Shi, Prof. S. Ostrovidov, Dr. X. Liang, Prof. K. Kurihara, Prof. K. Nakajima, Prof. H. Wu, Prof. A. Khademhosseini
WPI-Advanced Institute for Materials Research
Tohoku University
Sendai 980-8577, Japan
E-mail: chhkwwu@ust.hk; alik@rics.bwh.harvard.edu

Dr. Y. Zhao, Prof. H. Wu
Department of Chemistry and Division of Biomedical Engineering
Hong Kong University of Science and Technology
Hong Kong, China

Prof. M. Kasuya, Prof. K. Kurihara
Institute of Multidisciplinary Research for Advanced Materials
Tohoku University
Katahira, Aoba-ku
Sendai 980-8577, Japan

Prof. H. Bae, Prof. A. Khademhosseini
Department of Bioindustrial Technologies
College of Animal Bioscience and Technology
Konkuk University, Hwayang-dong, Kwangjin-gu
Seoul 143-701, Republic of Korea

Prof. A. Khademhosseini
Biomaterials Innovation Research Center
Department of Medicine
Brigham and Women's Hospital
Harvard Medical School
Cambridge, MA 02139, USA

Prof. A. Khademhosseini
Harvard-MIT Division of Health Sciences and Technology
Massachusetts Institute of Technology
Cambridge, MA 02139, USA

Prof. A. Khademhosseini
Wyss Institute for Biologically Inspired Engineering
Harvard University
Boston, MA 02115, USA

Prof. A. Khademhosseini
Department of Physics
King Abdulaziz University
Jeddah 21569, Saudi Arabia



DOI: 10.1002/adfm.201404531

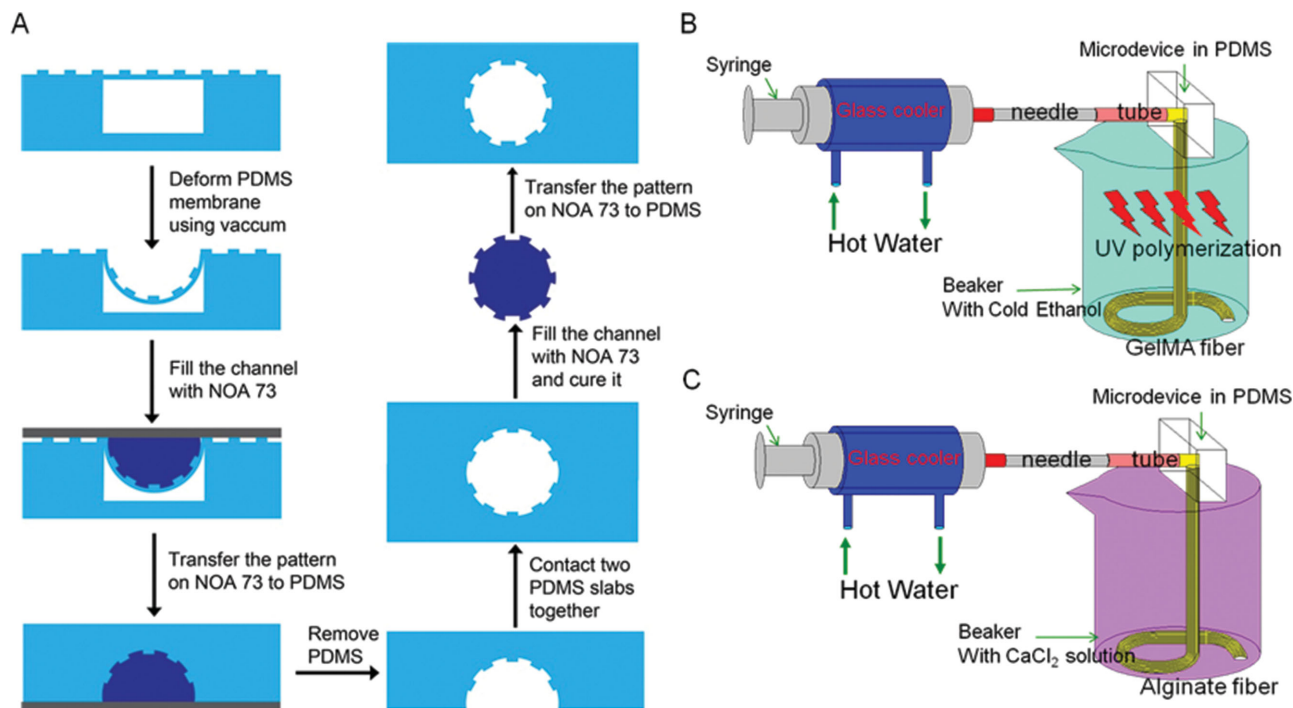


Figure 1. Schematic showing the fabrication process of the microdevice and its use to generate microstructured GelMA or alginate fibers, subsequently crosslinked by UV exposure and calcium ions, respectively.

bamboo-like, grooved, flat, porous, and tubular fibers).^[17–21] Previously, we have produced alginate microstructured fibers with specific spatial and compositional coding.^[18]

Although microfluidic techniques overcome the problem of generating fibers with a single morphology, the development of fibers with topographical architecture is still limited by the availability of suitable biomaterials. Due to its simple processing properties, alginate is the most commonly used material for generating fibers using microfluidic devices. However, alginate is not bioactive and lacks functionalities required to interact with cells.^[19–23] Although a number of studies have proposed to stimulate cell adhesion on alginate fibers by covalently linking various peptide sequences (e.g., RGD, KQAGDV, VAPG), this gel modification process is complex and time consuming, and peptides are expensive.^[24,25] Coating alginate hydrogels with polylysine, fibronectin, or laminin is an alternative approach to inducing cell adhesion.^[17,26–28] However, these coatings are temporary and unstable in cell culture conditions. Additionally, alginate fibers exhibit poor degradation characteristics, which may not be suitable for all applications. Therefore, research on new materials that facilitate desirable cell–material interactions and are amenable to easy fiber shape processing is of great interest. To this end, methacrylamide-modified gelatin (GelMA) may be a useful material for creating bioactive and biodegradable fibers that can not only promote cell adhesion but also enable cell encapsulation while maintaining high cell viability. GelMA can be photocrosslinked by light irradiation in the presence of a water-soluble photoinitiator to form hydrogels that are stable at 37 °C.^[29–33] Importantly, because GelMA is derived from gelatin (denatured collagen), it possesses many key properties of proteins from the extracellular matrix (ECM),

such as the ability to promote cell adhesion and proliferation and to be enzymatically degradable. Moreover, GelMA has stronger mechanical properties than natural ECM proteins, such as collagen.^[34–36] In particular, GelMA has been shown to possess high flexibility and excellent processability.^[37] Thus, it has been successfully micropatterned into various shapes and configurations for tissue engineering applications.^[38,39]

In this study, we propose the use of GelMA hydrogel as a biomaterial for the generation of photocrosslinkable microstructured fibers with microgroove patterns, formed using a facile microfluidic-based process. We investigated the morphology, mechanical properties, and processability of the prepared GelMA fibers. Furthermore, cell encapsulation in GelMA fibers and cell adhesion on GelMA fibers were evaluated and compared with similar groove-microstructured alginate fibers used as controls. In addition, a coculture model combining cell encapsulation and cell adhesion on the same fiber was developed. This advanced integration of GelMA and microfluidic technology has enabled the creation of photocrosslinkable bioactive, biodegradable, and cell-loaded microscale fibers with spatial micropatterns. We believe that the proposed microstructured GelMA fibers can be exploited to mimic various fibrous tissues and organs for potential applications in regenerative medicine.

2. Results and Discussion

2.1. Generation of Microstructured GelMA Fibers

As illustrated in **Figures 1** and **2A**, GelMA fibers ($\approx 500 \mu\text{m}$ in diameter) engraved with grooves ($\approx 20 \mu\text{m}$ width and height)

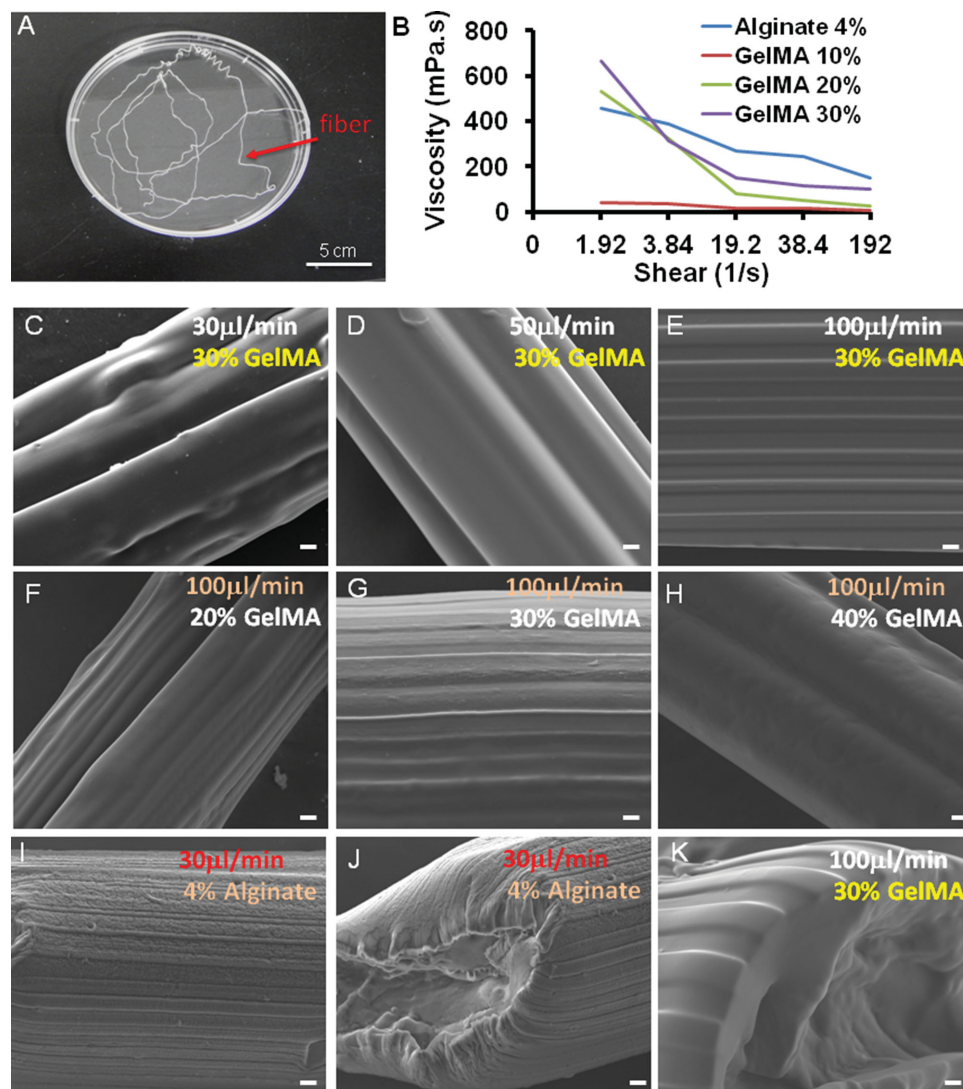


Figure 2. A) Photograph of a 30% GelMA microstructured fiber produced using the microdevice. B) Viscosity measurements of 10%, 20%, and 30% GelMA and 4% alginate solutions. C–K) FE-SEM images of microstructured GelMA fibers generated with a fixed concentration of 30% GelMA and different flow rates, C–E) a fixed flow rate at $100 \mu\text{L min}^{-1}$, and F–H) different GelMA concentrations. I) FE-SEM images of 4% alginate fiber generated at $30 \mu\text{L min}^{-1}$ and J) its cross-section. K) Cross-section of 30% GelMA fiber generated at $100 \mu\text{L min}^{-1}$. Scale bars indicate $20 \mu\text{m}$.

were continuously generated using a polydimethylsiloxane (PDMS)-based microfluidic device consisting of a grooved cylindrical channel ($20 \mu\text{m}$ in groove width and height). To facilitate the generation of continuous GelMA fibers, a thermal insulation system (i.e., a hot water circulating chamber) was used to maintain the temperature of the aqueous GelMA solution in the syringe at $60 \text{ }^\circ\text{C}$ before injection into the microdevice. Indeed, similar to gelatin and other natural polymers, a GelMA solution in pure water will gel at low temperatures, clogging the syringe and needle. A digital pump was used to control the flow of fluid injected into the microdevice. When the GelMA solution flowed from the microdevice outlet into cold ethanol (held at $-21 \text{ }^\circ\text{C}$ for 15 min), the low temperature induced immediate solidification of the formed GelMA fiber, which maintained its morphology molded by the grooved cylindrical channel of the microdevice.

After validating the feasibility of fiber generation with our microdevice, we optimized the generation of fine groove microstructures on GelMA fibers using different fluid flow rates and GelMA concentrations. Because the viscosity of GelMA solutions is of great importance for the generation of fibers with high-resolution microstructures, viscosities of aqueous GelMA solutions at different concentrations were measured and quantitatively analyzed using a cone-plate viscometer. Because a 4% (w/v) alginate solution in water is considered an excellent material for fabricating microstructured fibers, we used this formulation as a control.^[18–20] Figure 2B shows the viscosity plots of 10% (w/v), 20% (w/v), and 30% (w/v) aqueous GelMA solutions and 4% (w/v) aqueous alginate solution. The 30% (w/v) and 20% (w/v) GelMA solutions exhibited higher viscosity values at low shear rates. Their viscosities decreased significantly when the shear rate was more than $19.2 (1 \text{ s}^{-1})$. The 20% (w/v) GelMA

solution exhibited a greater viscosity decrease compared with the 30% (w/v) GelMA solution, whereas the 4% (w/v) alginate solution exhibited an average decrease in viscosity with the shear rate. Since the viscosity curve of 30% (w/v) GelMA was the most similar to that of 4% (w/v) alginate, we used a 30% GelMA solution to investigate the fiber generation at different flow rates.

The groove microstructure formation on GelMA fibers was investigated at flow rates of 30, 50, and 100 $\mu\text{L min}^{-1}$ (channel diameter 500 μm). The morphologies of the resulting fibers were recorded using field emission-scanning electron microscopy (FE-SEM; Figure 2C–E). Only unrefined groove microstructures (Figure 2C,D) were obtained at slow flow rates (30 and 50 $\mu\text{L min}^{-1}$). In contrast, fibers fabricated at flow rates of 100 $\mu\text{L min}^{-1}$ had well-defined groove patterns on their surfaces (Figure 2E).

GelMA fibers were fabricated using a flow rate of 100 $\mu\text{L min}^{-1}$ and different concentrations of GelMA to confirm the results of the viscosity tests. As shown in Figure 2F–H, fibers generated with 30% (w/v) GelMA presented surfaces with uniform and well-arranged grooves (Figure 2G,K cross section). The GelMA fiber diameter was ≈ 500 μm , whereas the groove width and height were ≈ 26 μm , which is slightly different from the size of grooved micropatterns (20 μm) used to produce the device. In contrast, due to their higher viscosity, fibers fabricated with 40% (w/v) GelMA exhibited a thicker surface with few grooves and large ridges (Figure 2H). Fibers fabricated with 20% (w/v) GelMA had an intermediate surface topography with visible grooves (Figure 2F). With a 10% (w/v) GelMA solution, the GelMA concentration was not sufficiently high to permit consistent fiber formation (data not shown). Therefore, a GelMA concentration of 30% (w/v) and a flow rate of 100 $\mu\text{L min}^{-1}$ were used to generate fibers in subsequent studies. Alginate 4% fibers (Figure 2I,J cross section) exhibited fine and regular groove microstructures and were used as controls in the following experiments. However, at the difference of GelMA fibers, alginate fibers usually presented a groove size ranging from 10 to 15 μm (width). This shrinkage in groove width may be correlated to the polymer nature and to the crosslinking steps, which are different for GelMA and alginate fibers. The swelling (and contraction) is an important property of hydrogels, which can be characterized by the polymer concentration, the mesh size, and their content in water.^[40] In general, as the crosslinking density increases the pore size of the hydrogel decreases, which decreases the swelling ratio.^[41,42]

2.2. Processability and Mechanical Properties of Microstructured GelMA Fibers

An important advantage of fibrous structures is their excellent processability, which allows them to be intertwined or knitted

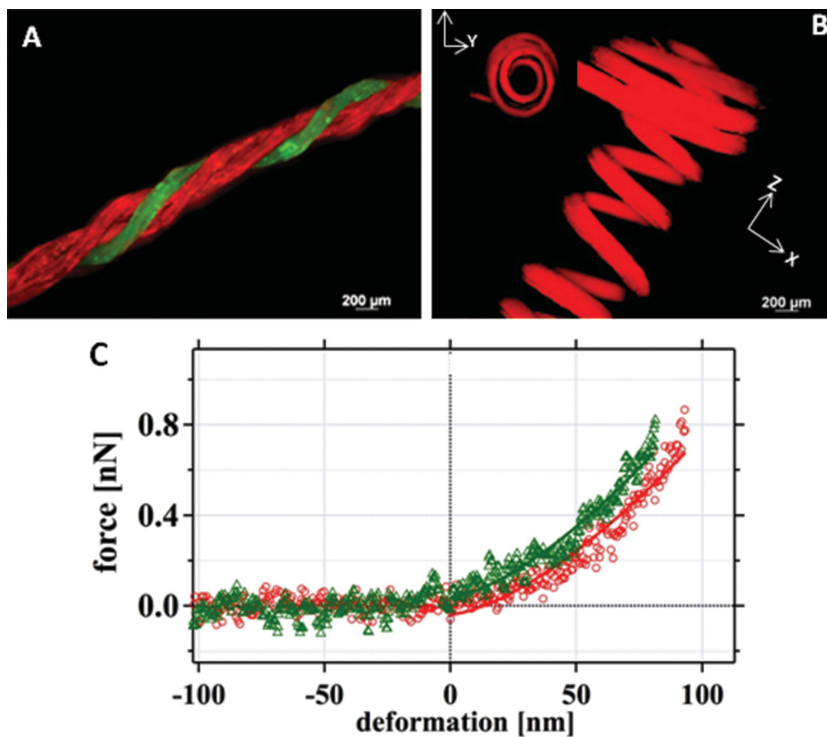


Figure 3. Processability and mechanical properties of 30% GelMA microstructured fibers. A,B) Fluorescent images of 30% GelMA microstructured fibers, loaded with 1% rhodamine (red) or FITC-dex 10 kDa (green), braided or wound. C) Force deformation curves for alginate (green) and GelMA (red) fibers obtained by AFM measurements.

(by hand or machine) into various 2D or 3D motifs.^[22] We investigated the processability of microstructured GelMA fibers before crosslinking with UV. GelMA 30% solutions were loaded with 1% fluorescent dyes (rhodamine (red) or fluorescein isothiocyanate-labeled dextran 10 kDa (green)) to allow individual fibers to be distinguished under fluorescence microscopy. As shown in Figure 3A,B, it was possible to generate various microarchitectural motifs (e.g., braids or springs) by manually winding or braiding GelMA fibers. The fibers did not break when tightened, intertwined, or braided. The fibers were then photocrosslinked under 7 mW cm^{-2} UV light for 2 min to preserve the generated motifs. We also analyzed the mechanical properties of GelMA fiber using atomic force microscopy (AFM; Figure 3C). For a GelMA 30% fiber, the Young's modulus, extracted from the force-deformation curve, was 8.9 kPa, close to that of alginate 4% fiber (9.6 kPa), which can be easily processed into various shapes by winding or braiding, as shown in several studies.^[18,19]

2.3. Cell Alignment on Microstructured GelMA Fibers

Cell alignment is an important parameter when engineering biological tissue, such as blood vessels or muscle.^[38] For example, in muscle engineering, the myoblast alignment promotes end-to-end connections between myoblasts, which favors myotube formation during the differentiation process.^[43] Moreover, the alignment of the formed myotubes toward one

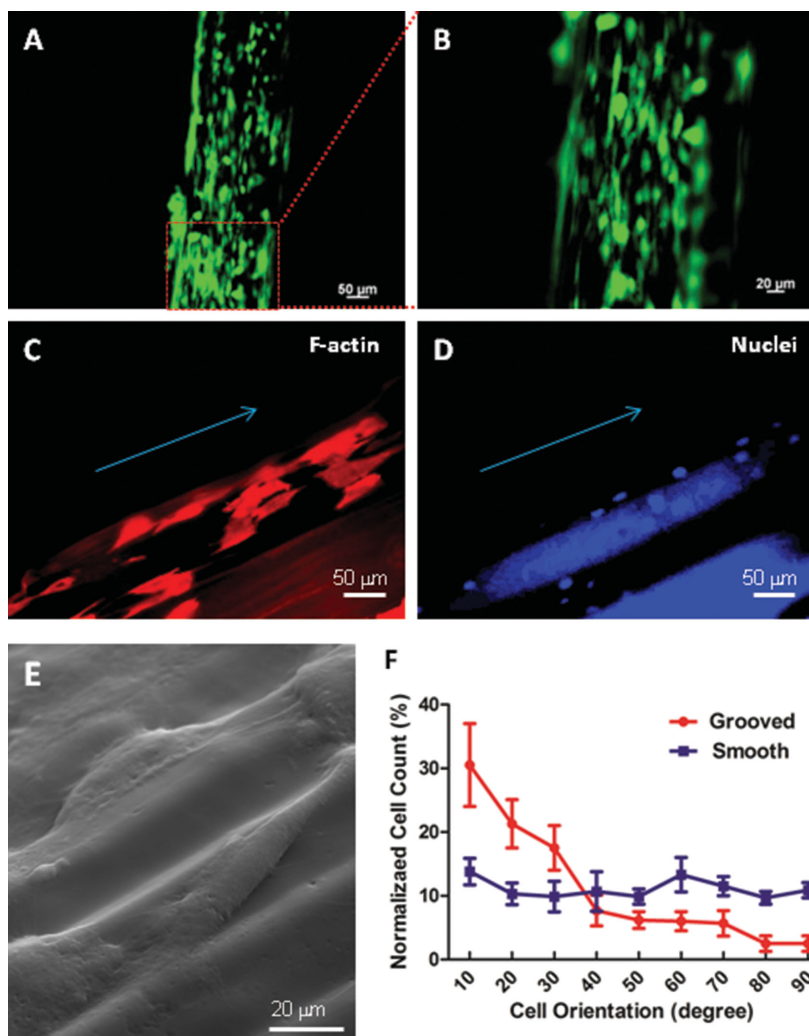


Figure 4. Cell alignment induced by the grooved/ridged microstructure on GelMA fibers. A,B) Fluorescent images of living cells (green) stained with Calcein AM at day 3 of culture. No dead cells (red) stained with ethidium homodimer-1 were observed. C,D) Fluorescent images showing cells orientation of F-actin (red) and cell nuclei (blue) stained, respectively, with Alexa Fluor 546-phalloidin and DAPI. E) FE-SEM image showing the cell colonization and alignment along the grooves of the GelMA fiber. F) Cell alignment quantification for cells cultured on 30% GelMA microstructured fibers and 30% GelMA fibers with smooth surfaces. Error bars represent standard error.

direction plays an important role in the total force produced by the engineered muscle.^[44] Therefore, we evaluated the cell alignment induced by the groove microstructure of GelMA fibers. C2C12 cells were seeded on the surfaces of microstructured GelMA fibers, and after three days of culture, the cells were stained with Live/Dead assay, Alexa Fluor 546-phalloidin, and DAPI to visualize, respectively, the cell viability, the F-actin, and cell nuclei under fluorescence microscopy. As shown in **Figure 4A–D**, C2C12 cells elongated along the fiber direction. This result was confirmed by FE-SEM analysis and **Figure 4E** reveals that myoblasts at the start of the culture initially colonized the grooves and elongated along the groove direction. Cell alignment was quantified for cells cultured for three days on microstructured GelMA fibers and cells cultured on smooth surface GelMA fibers. **Figure 4F** shows the cell alignment

quantification at 10° increments. ≈31% of cells cultured on microstructured GelMA fibers were aligned within 10°, whereas only 13% of cells cultured on smooth surface GelMA fiber were aligned.

2.4. Cell Adhesion and Encapsulation

Hydrogels are well suited for cell encapsulation and tissue engineering applications due to their viscoelastic properties and high hydration. However, cell adhesion is critical for maintaining the normal function of a tissue and plays essential roles in cell motility, proliferation, and differentiation.^[45,46] For anchorage-dependent cells, such as human umbilical vein endothelial cells (HUVECs) and fibroblasts, a solid substratum is required for adhesion and growth.^[47–49] Construction of a living tissue, such as a vessel or muscle, using hydrogel fibers requires that the fibers promote cell adhesion.^[50,51] In this study, both cell adhesion and encapsulation were evaluated for GelMA fibers. First, murine C2C12 myoblast cells and human osteoblasts (hFOBs) were encapsulated at high cell density (12×10^6 cells in 1 mL solution) in both microstructured GelMA fibers and microstructured alginate fibers (control). For seven days of culture, C2C12 myoblast cells encapsulated in fibers were stained for a viability assay and analyzed by fluorescence microscopy. As shown in **Figure 5A,B**, there were significantly more live cells (green) and significantly fewer dead cells (red) in GelMA fibers compared with alginate fibers. These results were also confirmed by a quantitative assay using a cell counting kit (**Figure 5C**). Viabilities of cells encapsulated in GelMA fibers were not significantly different from those encapsulated in alginate fibers at day 1 of culture. However, at day 7 of culture, both hFOBs and C2C12 myoblasts encapsulated in GelMA fibers exhibited remarkably higher cell viabilities compared with those of cells encapsulated in alginate fibers. Moreover, C2C12 cells encapsulated in GelMA fibers and cultured in low serum culture medium for seven days were able to differentiate into myotubes, as shown in **Figure 5D**.

Next, hFOBs, C2C12 myoblasts, and HUVECs were seeded on GelMA fibers and fibronectin-coated alginate fibers (i.e., alginate fibers treated with a $50 \mu\text{g mL}^{-1}$ fibronectin solution for 30 min). After seven days of culture, C2C12 myoblasts seeded at low cell density (2×10^4 cells cm^{-1} fiber) on fiber surfaces were stained with the viability kit. Only few viable cells still attached on alginate fibers (**Figure 6A**). In contrast, a large number of viable cells were observed on GelMA fibers, which proliferated and colonized the fiber surface (**Figure 6B**). Quantification of the cell numbers on the different fiber types for a long culture

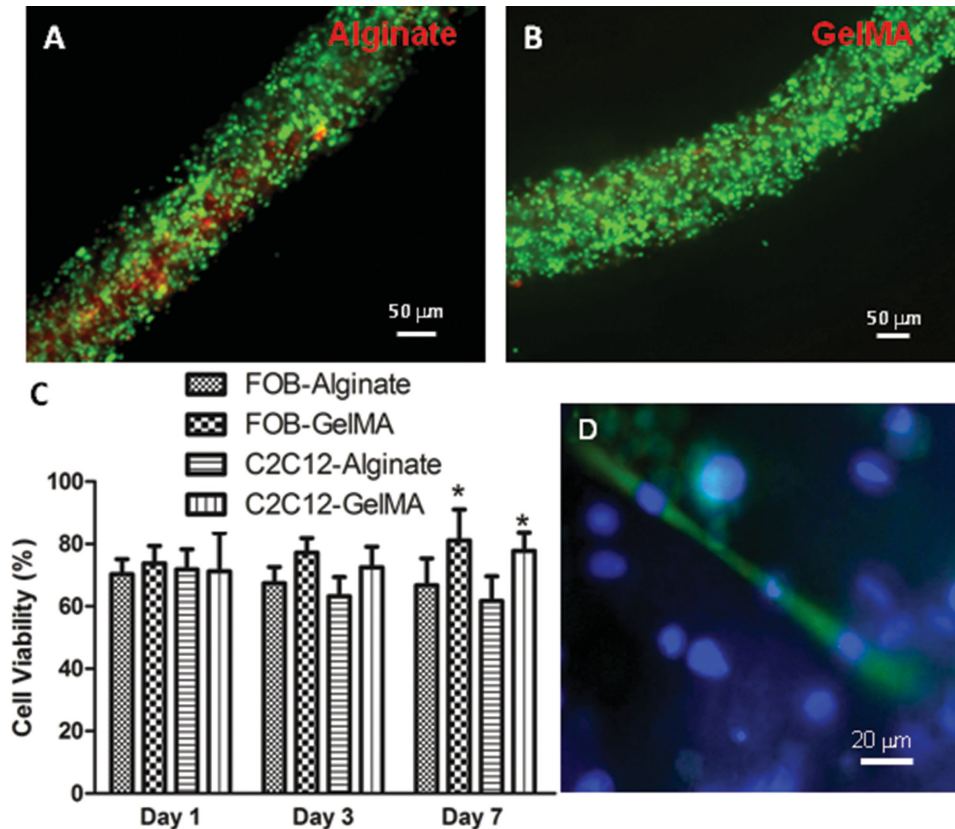


Figure 5. Viability of cells encapsulated in 30% GelMA microstructured fibers. A, B) Fluorescent images of C2C12 myoblast cells encapsulated at high cell density (12×10^6 cells in 1 mL solution) in 30% GelMA and 4% alginate fibers stained with Calcein AM (living cells, green) and ethidium homodimer-1 (dead cells, red) at day 7 of culture. C) Cell viability quantification at different days of culture for two different types of cells encapsulated in 30% GelMA and 4% alginate fibers. * indicates a significant difference when compared with cells cultured in alginate fibers ($p < 0.05$). D) Fluorescent image of myotube encapsulated into GelMA fiber at day 7 of culture in low serum culture medium, stained with mouse antifast skeletal myosin (MY-32) antibody, goat antimouse IgG antibody conjugated Alexa Fluor 488, and DAPI.

time (Figure 6C) showed that the number of living hFOBs, C2C12 myoblasts, and HUVECs adhered on GelMA fibers were significantly higher than those on alginate fibers after one day of culture. Cell adhesion on GelMA and alginate fibers significantly increased and decreased, respectively, after seven days of culture. Decreased cell adhesion on alginate fibers may be correlated with the instability of the fibronectin coating over time. hFOBs, C2C12 myoblasts, and HUVECs adhered on GelMA fibers were ≈ 11 -, 13-, and 12-fold higher, respectively, compared with those on alginate fibers after 12 days of culture.

Figure 6D shows gene expressions of genes correlated to cell attachment for C2C12 cells cultured on microstructured GelMA and alginate fibers relative to control cells cultured in a Petri dish. Among the different integrins involved in cell attachment to the ECM, those with $\beta 1$ subunits are involved in myoblast–myoblast fusion.^[52] The $\beta 1$ mRNA expression level in cells cultured on GelMA fibers was slightly higher than those of cells cultured in Petri dishes and significantly higher than those of cells cultured on alginate fibers. Talin is a cytosolic adapter protein that is concentrated in focal adhesions and links the intracellular domain of integrins to the actin cytoskeleton via association with vinculin. Therefore, its expression is indicative of cell adhesion strengthening.^[53] Talin mRNA expression was significantly higher in cells cultured on GelMA

fibers compared with those in control cells and cells cultured on alginate fibers. Moreover, collagen type 1 mRNA expression was also significantly higher in cells cultured on GelMA fibers compared with those in control cells on Petri dishes and cells cultured on alginate fibers. Therefore, the secretion of collagen by cells was improved, which indicated increased cell–substrate interactions with an increase in ECM protein deposition, providing additional mechanical strength and adhesive sites.^[54] Focal adhesion kinase (FAK) is a key tyrosine kinase involved in β integrin-mediated signal transduction.^[55] FAK mRNA expression was also higher when C2C12 cells were cultured on GelMA fibers than on Petri dishes and significantly higher than in cells cultured on alginate fibers. Taken together, these whole gene expression results indicated a higher activation of genes correlated to cell attachment when C2C12 cells were cultured on microstructured GelMA fibers compared with cells cultured on microstructured alginate fibers or Petri dishes, confirming superior cell–material interactions generated by GelMA.

Finally, a cell coculture model was also developed in this work (Figure 7A–C). Here, HUVECs (stained with red CellTracker) were encapsulated in microstructured GelMA fibers. Then, C2C12 myoblasts (stained with green CellTracker) were seeded on the surface of the HUVEC-laden GelMA fibers after one day of culture. This coculture model could facilitate

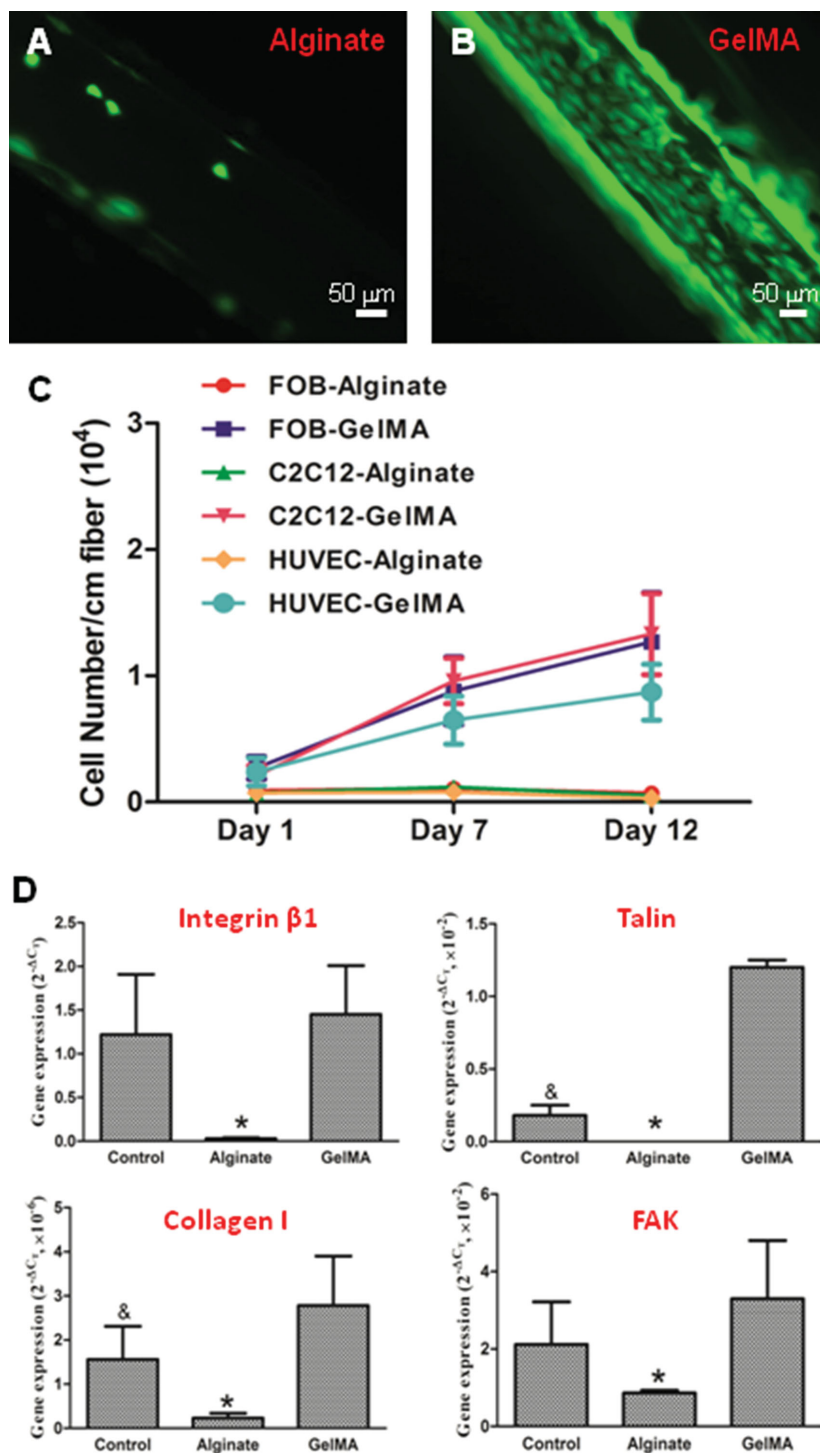


Figure 6. Viability of cells cultured on 30% GelMA microstructured fibers and expression of genes correlated to cell adhesion. A,B) Fluorescent images of C2C12 myoblast cells cultured on 30% GelMA fibers and 4% alginate fibers (coated with fibronectin) stained with Calcein AM (living cells, green) and ethidium homodimer-1 (dead cells, red) at day 7 of culture. C) Cell number quantification at day 1, day 7, and day 12 of culture for three different types of cells cultured on 30% GelMA and 4% alginate fibers (coated with fibronectin). D) Gene expression analysis of C2C12 cultured on microstructured 30% GelMA, fibronectin-coated 4% alginate fibers, and Petri dishes (used as a control) after five days of culture. Results were normalized to GAPDH ($p < 0.05$). * and & indicate significant differences when compared with gene expression of cells cultured on GelMA fibers and control, respectively ($p < 0.05$).

the construction of complicated tissues and organs requiring the assembly of multiple cell types, such as blood vessels, which are assembled with vascular smooth muscle cells and endothelial cells.^[56–60]

3. Conclusion

In summary, photocrosslinkable microstructured GelMA fibers with excellent cell-responsive properties and processability were fabricated using a microfluidic device. The generated fibers had well-defined grooved morphologies on their surface, which efficiently directed the alignment of cells grown on the fibers, favoring anisotropic tissue formation. Additionally, the fibers could be handled with ease, were sufficiently strong mechanically to exhibit excellent processability, and could be intertwined into a variety of motifs. Moreover, the microstructured GelMA fibers displayed a unique ability to promote cell adhesion and cell encapsulation. The biocompatibility of GelMA was excellent. Cells adhering to or encapsulated in microstructured GelMA fibers exhibited significantly higher cell viability compared with cells interacting with microstructured alginate fibers. Therefore, these findings suggest that microstructured GelMA fibers have excellent promise in tissue engineering applications, such as scaffolds to promote cell–material interactions for engineering blood vessels, muscle, or skin.

4. Experimental Section

Materials: Type A gelatin (from porcine skin), methacrylic anhydride, penicillin/streptomycin, alginate sodium salt, calcium chloride dehydrate, and sodium chloride were purchased from Sigma-Aldrich (USA). Ethanol was purchased from Kanto Chemical (Japan). Fetal bovine serum (FBS) was purchased from BioWest (USA). Photoinitiator (2-hydroxy-1-(4-(hydroxyethoxy)phenyl)-2-methyl-1-propanone (Irgacure 2959) was purchased from Ciba Chemicals (Japan). An Aladdin syringe pump was purchased from World Precision Instruments (Sarasota, FL, USA), and a glass chemical cooler was made inhouse. Dulbecco's modified Eagle's medium/F12 (DMEM/F12), DMEM, and Dulbecco's phosphate-buffered saline (DPBS) were purchased from Invitrogen (USA). For endothelial cell culture, an EGM-2 Bullet Kit (cc3162) was purchased from Lonza (USA). All chemicals were used without further purification. hFOB and C2C12 cell lines were purchased from American Type Culture Collection (ATCC; USA), and HUVECs were purchased from Lonza (USA). Cell assay kits were purchased from Invitrogen (USA).

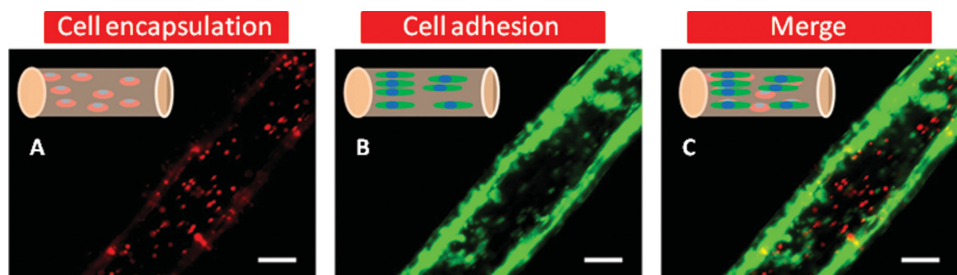


Figure 7. Fluorescent images of two different cell types cocultured using a 30% GelMA microstructured fiber. A) Fluorescent image of HUVECs (stained with red CellLinker PKH26) encapsulated in a microstructured GelMA fiber. B) Fluorescent image of C2C12 myoblasts (stained with green CellLinker PKH67) seeded on the surface of the HUVEC-laden GelMA fiber. C) Merged image of HUVECs and C2C12 myoblasts at day 1 of culture. Scale bars indicate 190 μm .

Fabrication of the Microfluidic Device for Fiber Generation: The microfluidic device was fabricated using a method described in the literature.^[18] Figure 1 shows a schematic of the process used to fabricate the device. Briefly, PDMS prepolymer (TSE3032, Momentive, Japan) was cured at 80 °C for 2 h to produce a thin PDMS membrane with grooved micropatterns (with a groove width and height of 20 μm) on an SU-8 master mold fabricated by conventional photolithography.^[61,62] This thin PDMS membrane with grooves was bonded to a PDMS mold with a channel using oxygen plasma for 10 s. The flat PDMS membrane was then deformed by vacuum into a concave hemicylindrical channel. This concave, hemicylindrical channel with grooved walls was filled with Norland Optical Adhesive 73 (NOA73). A second PDMS slab with a concave, hemicylindrical channel and grooved walls was generated using the same method, and the two PDMS slabs were pressed tightly together to generate a cylindrical channel with grooved walls. The cylindrical channel was filled with NOA73 and then photocrosslinked using UV light (365 nm) for 30 min to generate an NOA73 master mold after removal of the PDMS slabs. This NOA73 fiber mold with microstructured grooves was then used to generate PDMS devices with grooved cylindrical channels.

GelMA Synthesis: Gelatin type A (12 g) was dissolved in warm DPBS (120 mL) at 50 °C. The acrylation reaction took place under stirring for 1 h after the addition of 24 mL of methacrylic anhydride to the reaction mixture. The reaction was then stopped by dilution with 480 mL of warm (40 °C) DPBS. The resulting mixture was dialyzed for one week against warm distilled water (40 °C) using 12–14 kDa cutoff dialysis tubing and then lyophilized for one week.^[33,63]

Generation of Microstructured GelMA Fibers: To generate GelMA hydrogel fibers with microstructured patterns, we prepared a 30% (w/v) solution of GelMA in Milli-Q water at 60 °C with 3% photoinitiator (Irgacure 2959). The GelMA solution (held at 60 °C using a glass chamber perfused with hot water) was injected at 100 $\mu\text{L min}^{-1}$ into a microfluidic device consisting of a channel with grooved/ridged microstructured walls. The resulting microstructured fiber was harvested in cold ethanol (−21 °C for 15 min), transferred to a dish and subjected to 90 s of UV irradiation at 7 mW cm^{-2} (HayashiUL-410 UV-1, Hayashi Electronic Shenzhen Co., Ltd., Japan) for photocrosslinking.

Generation of Microstructured Alginate Fibers: To generate alginate hydrogel fibers with microstructured patterns, we prepared a 4% (w/v) solution of alginate in Milli-Q water at room temperature. The alginate solution (at room temperature) was injected at 30 $\mu\text{L min}^{-1}$ into the same microfluidic device consisting of a channel with grooved/ridged microstructured walls. The resulting microstructured fiber was harvested in an aqueous solution of 10% (w/v) calcium chloride dihydrate. The microstructured alginate fiber was kept for 20 min in a calcium chloride dihydrate solution for crosslinking.

Viscosity Measurements: The viscosities of GelMA (10% (w/v), 20% (w/v), and 30% (w/v)) and alginate (4% (w/v)) solutions were recorded using a programmable digital RVDV-II+ Pro viscometer (Brookfield) equipped with a 24 mm-diameter cone plate. The gap between the plates was 0.013 mm. When measuring the viscosity of GelMA solutions, a

water bath was used to maintain the temperature at 60 °C when the GelMA solutions were added to the lower plate.

Morphology of GelMA Microstructured Fibers: The morphologies of the microgrooved GelMA fibers were evaluated using a FE-SEM (JFC1600, JEOL, Tokyo) after platinum metallization in a sputter coater (30 s, 10 mA).

Cell Culture and Seeding: Alginate fibers in 40 mm-diameter dishes were treated with 5 mg mL^{-1} fibronectin for 30 min prior to cell seeding. HUVECs (passage 5) were cultured in supplemented EBM-2 culture medium (EGM-2 BulletKit). Murine C2C12 myoblasts (between passages 5 and 8) were cultured in DMEM supplemented with 10% FBS and 1% streptomycin/penicillin. Human osteoblasts (hFOBs, passage 3) were cultured in DMEM/F12 supplemented with 10% FBS and 1% streptomycin/penicillin. HEPES (20×10^{-3} M) was used to regulate the pH of the cell culture media at 7.4. HUVECs, C2C12 myoblasts, and hFOB were seeded on the GelMA and alginate fibers (2×10^4 cells cm^{-1} fiber) and incubated for 1 h to allow for cell attachment. 1 mL of culture medium was subsequently added.

Cell Encapsulation: HUVECs, C2C12 myoblasts, and hFOB (12×10^6) were mixed with 4% (w/v) alginate solution or 30% (w/v) GelMA solution (1 mL), respectively. Microstructured alginate or GelMA fibers with encapsulated cells were generated using the same method described above. However, GelMA fibers loaded with cells were harvested in cold DPBS (−21 °C for 10 min) and photocrosslinked under 90 s of UV irradiation at 7 mW cm^{-2} , while alginate fibers loaded with cells were harvested in cold aqueous solution of 10% CaCl_2 plus 0.9% NaCl and crosslinked for 10 min in this solution. Moreover, cells in warm GelMA solution were immediately processed.

Cell Coculture: 3×10^6 HUVECs were mixed with 30% (w/v) GelMA solution (1 mL). GelMA fibers with encapsulated cells were generated using the same method described above. C2C12 myoblasts (1×10^5 cells cm^{-1} fiber) were seeded on GelMA fibers with encapsulated HUVECs and incubated for 1 h to allow for cell attachment on the fibers. 1 mL of cell culture medium used for HUVEC cells was subsequently added.

Myotube Immunostaining: GelMA fibers with C2C12 cells encapsulated were cultured for seven days in low serum culture medium. Myotubes, defined as multinucleated cells having at least three cell nuclei, were fixed in the fiber with 4% (w/v) paraformaldehyde for 15 min, permeabilized with 0.3% (v/v) Triton X-100 for 5 min, blocked with 5% bovine serum albumin (BSA) in DPBS for 20 min at 37 °C, then incubated overnight at 4 °C with mouse monoclonal antifast skeletal myosin IgG antibody (abcam, code ab-7784, dilution 1:1000 in DPBS with 0.1% BSA). The next day, the samples were stained with Alexa fluor 488 conjugated goat antimouse IgG antibody (Invitrogen, code A11001, dilution 1:1000 in DPBS with 0.1% BSA) and incubated at 37 °C for 60 min. Photos were taken under a fluorescent microscope (Zeiss, Observer Z1, Germany).

Cell Viability and Morphology: The viabilities of C2C12 cells cultured on or encapsulated in microgrooved GelMA and alginate fibers were evaluated at one, three, and seven days after cell seeding using a Live/Dead Viability/Cytotoxicity kit (Invitrogen, USA). Calcein AM and ethidium homodimer-1 (EthD-1) were used to identify live and dead

Table 1. Primers and PCR conditions.

Primer name	Forward	Reverse
Integrin- β 1	5'-CAT CCC AAT TGT AGC AGG CG-3'	5'-CGT GTC CCA CTT GGC ATT CAT-3'
FAK	5'-GTA GTG AGC CAA CCA CCT GG-3'	5'-GCC CTT GTC TGT CAG GTA AC-3'
Talin	5'-GAA ATT GAG GCC AAG GTC CG -3'	5'-GCC TTC AGT CGT CTG TAC TG -3'
Collagen type 1	5'-ACT GGT ACA TCA GCC CGA AC -3'	5'-GGT GGA GGG AGT TTA CAC GA -3'
GAPDH (reference)	5'-TCA ACG GGA AGC CCA TCA-3'	5'-CTC GTG GTT CAC ACC CAT CA -3'

PCR conditions

Cycle 1: one time: 50 °C, 3 min; Cycle 2: one time: 95 °C, 5 min; Cycle 3: 40 times: (step 1 = 95 °C, 15 s; step 2 = 60 °C, 30 s); Cycle 4: one time: 40 °C, 1 min; Cycle 5: 81 times: 55 °C, 10 s.

cells, respectively. 1 μ L of calcein AM and 2 μ L of EthD-1 mixed in 1 mL of DPBS were added to a Petri dish with a 1 cm-long fiber seeded with cells on or in the fiber. After 30 min, the fiber was washed three times with DPBS, and cells on or in the fiber were observed using fluorescence microscopy (Zeiss, Germany). The number of viable cells on or in the fibers was determined using a Cell Counting Kit-8 (Sigma-Aldrich, USA). Briefly, cell-loaded fibers were incubated in 100 μ L of FBS-free media containing 10 μ L of CCK-8 solution for 2 h in an incubator. The absorbance of the solution was then measured at 450 nm using a microplate reader (BioTek, USA), and the total cell number on or in the fibers was calculated according to calibration curves built with known numbers of viable cells. For the FE-SEM analysis of the cell shape on microgrooved GelMA fibers, the cell-loaded fibers were fixed with 4% (w/v) formaldehyde in DPBS (pH 7.4) for 30 min, dehydrated with a graded ethanol series (50%, 70%, 80%, 90%, 100%, and 100%; 5 min at each concentration), placed in t-butyl alcohol, frozen for 1 h at -80 °C and freeze-dried overnight. The morphology of the cells on the fibers was visualized using FE-SEM (JFC1600, JEOL, Tokyo) after platinum metallization in a sputter coater (30 s, 10 mA).

Quantification of the Cell Alignment: After three days of culture on microgrooved GelMA fibers, HUVECs were fixed and permeabilized using 4% (w/v) formaldehyde for 15 min followed by 0.1% (v/v) Triton X-100 for 5 min. The cells were stained with phalloidin-conjugated Alexa-Fluor 594 (Invitrogen, USA) and DAPI (Sigma-Aldrich, USA) to visualize F-actin and cell nuclei, respectively. The F-actin (red color) and cell nuclei (blue color) were then imaged using fluorescence microscopy (Zeiss, Germany). Cellular alignment was quantitatively evaluated based on the alignment angle, which was defined as the angle between the long axis of a nucleus considered as elliptical and the groove direction (200 nuclei were analyzed using ImageJ software package). Alignment angles were then categorized in 10° increments. Cells with alignment angles less than 10° were considered aligned.

Gene Expression: The total RNAs of C2C12 myoblasts cultured on GelMA fibers, fibronectin-coated alginate fibers, and Petri dishes were extracted and purified using a TRIzol Plus RNA purification kit (Sigma-Aldrich) according to the manufacturer's instructions. One-step qRT-PCR was run using a MyiQ2 two-color RT-PCR detection system (Bio-Rad, USA). The qRT-PCR reaction mixture consisted of SuperScript III RT/Platinum Taq Mix (Invitrogen), ROX (Invitrogen), primers, an RNA template, and DEPC-treated water (Invitrogen). Primer sequences were designed by Greiner Bio-One, Japan (Table 1).

Winding Fibers into Various Shapes: 1 mL of 30% (w/v) GelMA solution with 3% photoinitiator (Irgacure 2959) was mixed with 0.1 g of rhodamine or 0.1 g of fluorescein isothiocyanate-dextran (FITC-dex, 10 kDa) and then used to produce rhodamine-loaded or FITC-dex-loaded fibers. The generated fibers were wound or braided into different shapes, placed in a dish and subjected to 2 min of UV irradiation at 7 mW cm⁻² (HayashiUL-410 UV-1, Hayashi Electronic Shenzhen Co., Ltd., Japan) for photocrosslinking.

Mechanical Properties of the Fibers: The mechanical properties of the alginate and GelMA fibers were investigated by a nanomechanical

mapping technique using AFM (Bruker Co., USA). The samples were maintained in liquid chambers and measured using a probe with a 0.4 μ m radius and a 0.2 N m⁻¹ spring constant (SD-Sphere-CONT-S, Nanosensors Co., SED).

Statistical Analysis: Data are displayed as means \pm standard deviation, and each experiment was performed in at least triplicate. Student's t-test and analysis of variance (ANOVA) followed by Tukey's multiple comparison test were performed to analyze the differences between experimental groups.

Acknowledgements

X.S. and S.O. contributed equally to this work. This work was supported by the World Premier International Research Center Initiative (WPI) from MEXT, Japan. H.K.W. acknowledges the support of the Hong Kong RGC (GRF 604712 and HKUST11/CRF/12).

Received: December 22, 2014

Revised: January 20, 2015

Published online: February 26, 2015

- [1] M. Balter, *Science* **2009**, 325, 1329.
- [2] A. Hasan, A. Memic, N. Annabi, M. Hossain, A. Paul, M. R. Dokmeci, F. Dehghani, A. Khademhosseini, *Acta Biomater.* **2014**, 10, 11.
- [3] R. Murugan, S. Ramakrishna, *Tissue Eng.* **2007**, 13, 1845.
- [4] D. W. Huttmacher, *Biomaterials* **2000**, 21, 2529.
- [5] S. Zhang, X. Liu, S. F. Barreto-Oriz, Y. Yu, B. P. Ginn, N. A. DeSantis, D. L. Hutton, W. L. Grayson, F. Z. Cui, B. A. Korgel, S. Gerecht, H. Q. Mao, *Biomaterials* **2014**, 35, 3243.
- [6] M. P. Lutolf, J. A. Hubbell, *Nat. Biotechnol.* **2005**, 23, 47.
- [7] A. Tamayol, M. Akbari, N. Annabi, A. Paul, A. Khademhosseini, D. Juncker, *Biotechnol. Adv.* **2013**, 31, 669.
- [8] M. C. Serrano, E. J. Chung, G. A. Ameer, *Adv. Funct. Mater.* **2010**, 20, 192.
- [9] H. Kerdjoudj, C. Boura, V. Moby, K. Montagne, P. Schaaf, J. C. Voegel, J. F. Stoltz, P. Menu, *Adv. Funct. Mater.* **2007**, 17, 2667.
- [10] Y. Jun, E. Kang, S. Chae, S. H. Lee, *Lab Chip* **2014**, 14, 2145.
- [11] W. Liu, S. Thomopoulos, Y. Xia, *Adv. Healthcare Mater.* **2012**, 1, 10.
- [12] A. C. Wan, M. F. Leong, J. K. C. Toh, Y. Zheng, J. Y. Ying, *Adv. Healthcare Mater.* **2012**, 1, 101.
- [13] J. A. Cooper, H. H. Lu, F. K. Ko, J. W. Freeman, C. T. Laurencin, *Biomaterials* **2005**, 26, 1523.
- [14] E. Mathiowitz, D. M. Lavin, R. A. Hopkin, *Ther. Delivery* **2013**, 4, 1075.
- [15] B. Kundu, R. Rajkhowa, S. C. Kundu, X. Wang, *Adv. Drug Delivery Rev.* **2013**, 65, 457.

- [16] M. F. Leong, J. K. C. Toh, C. Du, K. Narayanan, H. F. Lu, T. C. Lim, A. C. A. Wan, J. Y. Ying, *Nat. Commun.* **2013**, *4*, 2353.
- [17] H. Onoe, T. Okitsu, A. Itou, M. Kato-Negishi, R. Gojo, D. Kiriya, K. Sato, S. Miura, S. Iwanaga, K. Kuribayashi-Shigetomi, Y. T. Matsunaga, Y. Shimoyama, S. Takeuchi, *Nat. Mater.* **2013**, *12*, 584.
- [18] E. Kang, G. S. Jeong, Y. Y. Choi, K. H. Lee, A. Khademhosseini, S. H. Lee, *Nat. Mater.* **2011**, *10*, 877.
- [19] M. Akbari, A. Tamayol, V. Laforte, N. Annabi, A. H. Najafabadi, A. Khademhosseini, D. Juncker, *Adv. Funct. Mater.* **2014**, *24*, 4060.
- [20] Y. Yu, J. Ma, S. Lykkemark, H. Xu, J. Qin, *Adv. Mater.* **2014**, *26*, 2494.
- [21] E. Kang, Y. Y. Choi, S. K. Chae, J. H. Moon, J. Y. Chang, S. H. Lee, *Adv. Mater.* **2012**, *24*, 4271.
- [22] S. K. Chae, E. Kang, A. Khademhosseini, S. H. Lee, *Adv. Mater.* **2013**, *25*, 3071.
- [23] J. Su, Y. Zheng, H. Wu, *Lab Chip* **2009**, *9*, 996.
- [24] B. K. Mann, A. T. Tsai, T. Scott-Burden, J. L. West, *Biomaterials* **1999**, *20*, 2281.
- [25] B. K. Mann, R. H. Schmedlen, J. L. West, *Biomaterials* **2001**, *22*, 439.
- [26] A. Mosahebi, M. Wiberg, G. Terenghi, *Tissue Eng.* **2003**, *9*, 209.
- [27] M. Dvir-Ginzberg, T. Elkayam, S. Cohen, *Tissue Eng.* **2004**, *10*, 1806.
- [28] A. Thakur, R. Sengupta, H. Matsui, D. Lillicrap, K. Jones, G. Hortelano, *J. Biomed. Mater. Res. B* **2010**, *94*, 296.
- [29] E. Kaemmerer, F. P. Melchels, B. M. Holzapfel, D. W. Hutmacher, D. Loessner, *Acta Biomater.* **2014**, *10*, 2551.
- [30] C. Cha, J. Oh, K. Kim, Y. Qiu, M. Joh, S. R. Shin, X. Wang, G. Camci-Unal, K. T. Wan, R. Liao, A. Khademhosseini, *Biomacromolecules* **2014**, *15*, 283.
- [31] S. R. Shin, B. Aghaei-Ghareh-Bolagh, T. T. Dang, S. N. Topkaya, X. Gao, S. Y. Yang, S. M. Jung, J. H. Oh, M. R. Dokmeci, X. S. Tang, A. Khademhosseini, *Adv. Mater.* **2013**, *25*, 6385.
- [32] Y. C. Chen, R. Z. Lin, H. Qi, Y. Yang, H. Bae, J. M. Melero-Martin, A. Khademhosseini, *Adv. Funct. Mater.* **2012**, *22*, 2027.
- [33] H. Aubin, J. W. Nichol, C. B. Huston, H. Bae, A. L. Sieminski, D. M. Crokek, P. Akhyari, A. Khademhosseini, *Biomaterials* **2010**, *31*, 6941.
- [34] J. W. Nichol, S. T. Koshy, H. Bae, C. M. Hwang, S. Yamanlar, A. Khademhosseini, *Biomaterials* **2010**, *31*, 5536.
- [35] S. R. Shin, H. Bae, J. M. Cha, J. Y. Mun, Y. C. Chen, H. Tekin, H. Shin, S. Farshchi, M. R. Dokmeci, S. Tang, A. Khademhosseini, *ACS Nano* **2012**, *6*, 362.
- [36] M. Nikkhan, N. Eshak, P. Zorlutuna, N. Annabi, M. Castello, K. Kim, A. Dolatshahi-Pirouz, F. Edalat, H. Bae, Y. Yang, A. Khademhosseini, *Biomaterials* **2012**, *33*, 9009.
- [37] Y. Zuo, W. Xiao, X. Chen, Y. Tang, H. Luo, H. Fan, *Chem. Commun.* **2012**, *48*, 3170.
- [38] S. Ostrovidov, V. Hosseini, S. Ahadian, T. Fujie, S. P. Parthiband, M. Ramalingam, H. Bae, H. Kaji, A. Khademhosseini, *Tissue Eng. Part B* **2014**, *20*, 403.
- [39] B. M. Gumbiner, *Cell* **1996**, *84*, 345.
- [40] N. A. Peppas, P. Bures, W. Leobandung, H. Ichikawa, *Eur. J. Pharm. Biopharm.* **2000**, *50*, 27.
- [41] S. Ostrovidov, N. Annabi, A. Seidi, M. Ramalingam, F. Dehghani, H. Kaji, A. Khademhosseini, *Anal. Chem.* **2012**, *84*, 1302.
- [42] R. A. Scott, N. A. Peppas, *Biomaterials* **1999**, *20*, 1371.
- [43] M. T. Lam, Y.-C. Huang, R. K. Birla, S. Takayama, *Biomaterials* **2009**, *30*, 1150.
- [44] W. Bian, M. Juhas, T. W. Pfeiler, N. Bursac, *Tissue Eng. Part A* **2012**, *18*, 957.
- [45] C. R. Mackay, B. A. Imhof, *Trends Immunol.* **1993**, *14*, 99.
- [46] R. O. Hynes, *Trends Biochem. Sci.* **1999**, *24*, M33.
- [47] P. Premnath, B. Tan, K. Venkatakrishnan, *J. Biomed. Nanotechnol.* **2014**, *10*, 1061.
- [48] X. T. Shi, T. Fujie, A. Saito, S. Takeoka, Y. Hou, Y. Shu, M. Chen, H. Wu, A. Khademhosseini, *Adv. Mater.* **2014**, *26*, 3290.
- [49] X. T. Shi, S. Chen, J. Zhou, H. Yu, L. Li, H. Wu, *Adv. Funct. Mater.* **2012**, *22*, 3799.
- [50] J. M. Silva, A. R. C. Duarte, C. A. Custódio, P. Sher, A. I. Neto, A. C. M. Pinho, J. Fonseca, R. L. Reis, J. F. Mano, *Adv. Healthcare Mater.* **2014**, *3*, 433.
- [51] S. Ostrovidov, X. Shi, L. Zhang, X. Liang, S. B. Kim, T. Fujie, M. Ramalingam, M. Chen, K. Nakajima, F. Al-Hazmi, H. Bae, A. Memic, A. Khademhosseini, *Biomaterials* **2014**, *35*, 6268.
- [52] S. M. Hindi, M. M. Tajrishi, A. Kumar, *Sci. Signal* **2013**, *6*, re2.
- [53] F. J. Conti, S. J. Monkley, M. R. Wood, D. R. Critchley, U. Muller, *Development* **2009**, *136*, 3597.
- [54] P. Y. Wang, T. H. Wu, P. H. Chao, W. H. Kuo, M. J. Wang, C. C. Hsu, W. B. Tsai, *Biotechnol. Bioeng.* **2013**, *110*, 327.
- [55] N. L. Quach, T. A. Rando, *Dev. Biol.* **2006**, *293*, 38.
- [56] N. Annabi, A. Tamayol, J. A. Uquillas, M. Akbari, L. E. Bertassoni, C. Cha, G. Camci-Unal, M. R. Dokmeci, N. A. Peppas, A. Khademhosseini, *Adv. Mater.* **2014**, *26*, 85.
- [57] D. A. Wang, S. Varghese, B. Sharma, I. Strehin, S. Fermanian, J. Gorham, H. D. Fairbrother, B. Cascio, J. H. Elisseeff, *Nat. Mater.* **2007**, *6*, 385.
- [58] X. T. Shi, J. Zhou, Y. Zhao, L. Li, H. Wu, *Adv. Healthcare Mater.* **2013**, *2*, 846.
- [59] C. M. Wang, Y. H. Gong, Y. Zhong, Y. C. Yao, K. Su, D. A. Wang, *Biomaterials* **2009**, *30*, 2259.
- [60] D. A. Wang, C. G. Williams, Q. Li, B. Sharma, J. H. Elisseeff, *Biomaterials* **2003**, *24*, 3969.
- [61] S. Ostrovidov, J. Jiang, Y. Sakai, T. Fujii, *Biomed. Microdev.* **2004**, *6*, 279.
- [62] S. Ostrovidov, Y. Sakai, T. Fujii, *Biomed. Microdev.* **2011**, *13*, 847.
- [63] J. W. Nichol, S. T. Koshy, H. Bae, C. M. Hwang, S. Yamanlar, A. Khademhosseini, *Biomaterials* **2010**, *31*, 5536.